An Analytical High-Level Battery Model for Use in Energy Management of Portable Electronic Systems *

Daler N. Rakhmatov and Sarma B.K. Vrudhula
Center for Low Power Electronics
ECE Department, University of Arizona
Tucson, AZ 85721
daler/sarma@ece.arizona.edu

ABSTRACT

Once the battery becomes fully discharged, a battery-powered portable electronic system goes off-line. Therefore, it is important to take the battery behavior into account. A system designer needs an adequate high-level model in order to make battery-aware decisions that target maximization of the system's lifetime on-line. We propose such a model: it allows a designer to predict the battery time-to-failure for a given load and provides a cost metric for lifetime optimization algorithms. Our model also allows for a tradeoff between the accuracy and the amount of computation performed. The quality of the proposed model is evaluated using a detailed low-level simulation of a lithium-ion electrochemical cell.

1. INTRODUCTION

The lifetime, or *time-to-failure*, of the battery is the time when it becomes fully discharged. Once the battery is exhausted the system shuts down; therefore, maximizing the time-to-failure is an important problem. Our goal is to develop an analytical model of a generic battery that can be used for lifetime estimation and optimization under various loads.

A system designer can use such a model to evaluate alternative system loads and select the most battery-friendly one. For example, the task schedule and task execution parameters, such as the operating voltage and the clock frequency, can be chosen so that the battery drain is minimized. Also, a designer can take advantage of the charge *recovery* effect which takes place not only during the recharge periods but also during sleep periods. These off-line periods can be scheduled with the goal of maximizing system's lifetime on-line.

Modeling of batteries is difficult due to nonlinearities of charge delivery, especially when the load varies with time. The lifetime L under the *constant* load can be predicted based on empirical Peukert's relationship [7]: $a = I^b L$, where I is the current, and a and b are appropriate parameters. This power law does not hold for the *variable* load (the current is changing over time), when the current average does not adequately represent the battery discharge conditions. According to the Peukert's law, all load profiles with the same average would yield the same time-to-failure; however this conclusion contradicts experimental observations.

We propose a model that handles variable loads very well and provides a more accurate alternative to the Peukert's law for the constant loads. Our approach also permits a trade-off between the accuracy and the amount of computation performed. Moreover, the proposed relationship is *derived* based on the physical principles of the battery operation.

This paper is organized as follows. Section 2 provides a brief summary of the recent work in battery modeling. In Section 3 we derive the model, and in Section 4 we examine its behavior of the model under constant and time-varying discharge profiles. Section 5 describes applications of the proposed model, and Section 6 concludes the paper.

2. RELATED WORK

An outline of battery-related issues, faced by battery users designing portable electronics, are presented in [11, 13, 15]. For a battery user, it is important to know the battery behavior at the *macroscopic* scale. In other words, a user needs a model that captures the high-level essence of the battery operation. There already exist tools that allow for detailed analysis of the battery at the *microscopic* scale [5, 8]. However, such low-level models rely on a numerical simulation of partial differential equations describing complex electrochemical processes taking place inside the battery. As a result, such simulators are very slow, which makes faster high-level models a preferable choice from the CAD perspective. The high-level approach can be based on either simulating an equivalent representation of a battery [3, 9, 12], or some analytical expression relating load conditions to battery performance [6, 13, 16].

Several high-level simulation-based models have been reported: a PSPICE equivalent circuit [9], a discrete-time VHDL model [3], and a Markov chain [12]. In terms of the prediction accuracy and generality, the most successful approach is due to [12]: it is a Markov chain of the battery charge states with the forward transitions corresponding to discharge, and backward transitions corresponding to recovery. The load is expressed as a stochastic demand on charge units. If in a given time slot some number of charge units are "discharged", then an appropriate forward transition takes place (a loss of some charge). If in a given time slot no charge units are demanded, an appropriate backward transition takes place

*This work was carried out at the National Science Foundation's State/Industry/University Cooperative Research Centers' (NSF-S/IUCRC) Center for Low Power Electronics (CLPE). CLPE is supported by the NSF (Grant EEC-9523338), the State of Arizona, and a consortium of companies from the microelectronics industry (visit the CLPE web site http://clpe.ece.arizona.edu).

(a recovery of some charge). Thus, this stochastic model can account for both charge delivery nonlinearity and charge recovery effects. These simulators can serve as good estimation tools; however, unlike analytical models, they do not provide a formal cost function for lifetime optimizations. Also, parameter characterization for these simulators can be a difficult process.

Next, we briefly address related work on analytical modeling. The authors of [6] consider special cases of the discharge process: diffusion-limited, reaction-limited, and ohmically limited. They obtain relationships between the discharge rate and the battery capacity, providing valuable information to battery designers. The authors of [13] introduce the efficiency factor that accounts for charge delivery nonlinearity. They consider two approximations for the dependency of this factor on the battery load: linear and quadratic. The resulting model was relatively accurate with comparison to the PSPICE simulation results. The authors of [16] took a statistical approach. They obtained the battery voltage-time measurement data from several constant-load tests. Fitting of the voltage-time curves into a Weibull model showed a good approximation. Then, a relatively successful attempt was made to model the battery behavior over a range of constant loads; however, time-varying discharge was not considered. Inherently, these analytical models are not as accurate and general as the simulation-based models.

The model described in this paper overcomes the aforementioned drawbacks of the existing models. Our objective is to combine the accuracy and generality of a low-level simulation-based model and the high-level nature of an analytical model. We represent the real battery by a simplistic equivalent battery, and derive our analytical expression from the fundamental physical laws. There are only two unknown parameters that can be estimated based on several constant-load tests.

3. MODEL DESCRIPTION

Every battery has two electrodes, *cathode* and *anode*, which are separated by an *electrolyte*. During battery discharge, the anode releases electrons to an external circuit, and the cathode accepts electrons from the circuit. Thus, a loss of electrons (oxidation) at the anode is coupled with the gain of electrons (reduction) at the cathode. We assume that reduction at the anode and oxidation at the cathode are negligible. Then, the electrode reactions, involving ν electrons, oxidized species O, and reduced species R, can be represented as follows [2]:

$$\begin{array}{ll} O+\nu^- \rightarrow R & (cathode) \\ R \rightarrow O+\nu^- & (anode) \end{array} \tag{1}$$

In equilibrium (no load), electroactive spieces O and R are uniformly distributed in the electrolyte. Once the external flow of electrons is established, the number of species near the electrode decreases due to the electrochemical reaction. As a result, a nonzero concentration gradient is created across the electrolyte, and the laws of diffusion apply. If a load is switched off, then the concentration near the electrode surface starts increasing, or *recovering*, due to diffusion. Eventually, the spieces will become uniformly distributed in the electrolyte again; however, their concentration level will be lower than the initial value.

Once the concentration of O (R) near the cathode (anode) drops below a certain level, the reaction can no longer be sustained. Assuming that O and R behave in the same way, we do not differentiate between the electrodes. The time L when the reaction can no longer take place at the electrode surface *is* the time-to-failure in question.

We consider the simple case of one-dimensional diffusion in a finite region of some length w. Let $C(x,t)$ denote the concentration of species at time $t \in [0,L]$ at distance $x \in [0,w]$ from the electrode. We are interested in the concentration values $C(0,t)$ at the electrode surface ($x=0$). Let initial concentration $C(x,0)=C^*$ for all x, and let $\rho(t) = 1 - \frac{C(0,t)}{C^*}$. When $C(0,t)$ drops below the cutoff level C_{cutoff} at time $t=L$, the value of $\rho(L)$ crosses over the corresponding threshold $(1-\frac{C_{cutoff}}{C^*})$. It is an analytical expression for $\rho(t)$ that we want to find in order to compute the time-to-failure L.

Concentration behavior due to one-dimensional diffusion is described by the following Fick's laws [2]:

$$-J(x,t) = D\frac{\partial C(x,t)}{\partial x} \tag{2}$$

$$\frac{\partial C(x,t)}{\partial t} = D\frac{\partial^2 C(x,t)}{\partial x^2} \tag{3}$$

$J(x,t)$ denotes the flux of species at time t at distance x, and D denotes the diffusion coefficient. In accordance with the Faraday's law, the flux at the left boundary of the diffusion region (the electrode surface) is proportional to the current $i(t)$ (the external load applied) [2]. The flux at the right boundary of the diffusion region ($x=w$) is zero. Therefore, the following two conditions hold:

$$\frac{i(t)}{\nu FA} = D\frac{\partial C(x,t)}{\partial x}\bigg|_{x=0} \tag{4}$$

$$0 = D\frac{\partial C(x,t)}{\partial x}\bigg|_{x=w} \tag{5}$$

In equation 4, A is the area of the electrode, and F denotes the Faraday's constant ($96485.31\ C\ mol^{-1}$). Given these partial differential equations and boundary conditions, it is possible to obtain an analytical solution. Next, we present the main results of our derivations, omitting details.

Let $\bar{C}(x,s)$ and $\bar{i}(s)$ denote the Laplace transforms of $C(x,t)$ and $i(t)$, respectively. In the s-domain, the solution for the concentration at the electrode surface is as follows:

$$\bar{C}(0,s) = \frac{C^*}{s} - \frac{\bar{i}(s)}{\nu FAD}\frac{\coth(w\sqrt{\frac{s}{D}})}{\sqrt{\frac{s}{D}}} \tag{6}$$

Multiplication in the s-domain corresponds to convolution in the time-domain. The inverse Laplace transformation $\bar{C}(0,s) \rightarrow C(0,t)$ yields, due to [14],

$$C(0,t) = C^* - \frac{i(t)}{\nu FAD} * \sqrt{\frac{D}{\pi t}} \sum_{m=-\infty}^{\infty} e^{-\frac{w^2m^2}{Dt}} \tag{7}$$

$$1 - \frac{C(0,t)}{C^*} = \frac{1}{\nu FA\sqrt{\pi D}C^*} \int_0^t \frac{i(\tau)}{\sqrt{t-\tau}} \sum_{m=-\infty}^{\infty} e^{-\frac{w^2m^2}{D(t-\tau)}}\, d\tau \tag{8}$$

$$\rho(t) = \frac{1}{\nu FA\sqrt{\pi D}C^*} \int_0^t \frac{i(\tau)}{\sqrt{t-\tau}} \Big[1 + 2\sum_{m=1}^{\infty} e^{-\frac{w^2m^2}{D(t-\tau)}}\Big]\, d\tau \tag{9}$$

For $\tau \in [0,t]$, the series is uniformly convergent[1]; therefore, integration can be performed term by term. Then,

$$\rho(t) = \frac{1}{\nu FA\sqrt{\pi D}C^*} \Big[\int_0^t \frac{i(\tau)}{\sqrt{t-\tau}}\, d\tau + 2\sum_{m=1}^{\infty} \int_0^t \frac{i(\tau)}{\sqrt{t-\tau}} e^{-\frac{w^2m^2}{D(t-\tau)}}\, d\tau \Big] \tag{10}$$

[1]Note that $\tau \in [0,t] \Rightarrow \frac{w^2}{D(t-\tau)} > 0 \Rightarrow e^{-\frac{w^2m^2}{D(t-\tau)}} < 1\ \forall\ m \geq 1$. Since $|e^{-\frac{w^2(n+m)^2}{D(t-\tau)}} - e^{-\frac{w^2m^2}{D(t-\tau)}}| < 1\ \forall\ n,m \geq 1$, Cauchy criterion for convergence holds; therefore, the series is convergent.

Let $\beta = \frac{w}{\sqrt{D}}$, and $\alpha = \nu FA\sqrt{\pi D}C^*\rho(L)$. Then, one obtains the following general expression relating the load, the time-to-failure, and the battery parameters:

$$\alpha = \int_0^L \frac{i(\tau)}{\sqrt{L-\tau}}\, d\tau + 2\sum_{m=1}^{\infty} \int_0^L \frac{i(\tau)}{\sqrt{L-\tau}}\, e^{-\frac{\beta^2 m^2}{L-\tau}}\, d\tau \qquad (11)$$

3.1 Special case: constant load

For the special case of the constant discharge rate, let $i(t) = I$. In this case, the Peukert's law applies. We compare our alternative to the Peukert's law in terms of relative and absolute errors in lifetime predictions.

The constant I can be brought out of the integrals, and one obtains [10]:

$$\alpha = 2I\left\{\sqrt{L} + 2\sum_{m=1}^{\infty}\left[\sqrt{L}\, e^{-\frac{\beta^2 m^2}{L}} - \beta m\sqrt{\pi}\bar{\Phi}(\frac{\beta m}{\sqrt{L}})\right]\right\} \qquad (12)$$

In equation 12, $\bar{\Phi}(x) = 1 - \frac{2}{\sqrt{\pi}}\int_0^x e^{-y^2}\, dy$, which is the complementary error function. The following function [4] gives an excellent approximation for $\bar{\Phi}(x)$ over all nonnegative arguments:

$$\bar{\Phi}(x) \approx \frac{e^{-x^2}}{\sqrt{\pi}(x - \frac{x}{\pi} + \frac{\sqrt{x^2+\pi}}{\pi})} \qquad (13)$$

Then,

$$\beta m\sqrt{\pi}\bar{\Phi}(\frac{\beta m}{\sqrt{t}}) \approx \frac{\pi\sqrt{t}\, e^{-\frac{\beta^2 m^2}{t}}}{\pi - 1 + \sqrt{1 + \pi\frac{t}{\beta^2 m^2}}} \qquad (14)$$

In equation 12, we take only the first ten terms of the infinite series. Figure 1 shows plots of the approximated 10-term sum and the original 100000-term sum for the values of $\frac{\beta^2}{L}$ ranging from 0.01 to 5. Since the terms decrease very rapidly as m grows, the sum of the first ten terms is an excellent approximation of the entire infinite sum for $\frac{\beta^2}{L} \geq \frac{1}{100}$.

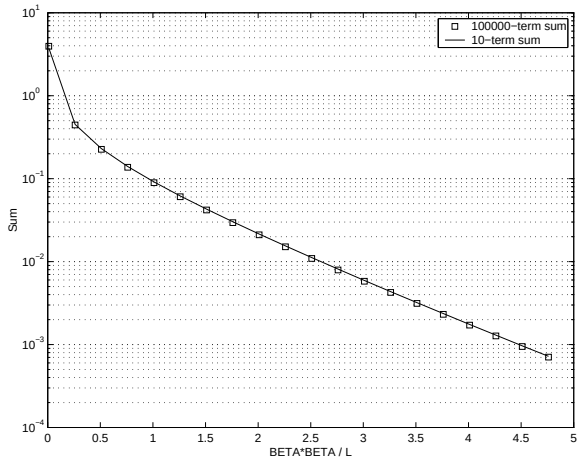

Figure 1: Approximation for Infinite Sum in Equation 12.

Thus,

$$\alpha = 2I\sqrt{L}\left[1 + 2\sum_{m=1}^{10}\left(e^{-\frac{\beta^2 m^2}{L}} - \frac{\pi\, e^{-\frac{\beta^2 m^2}{L}}}{\pi - 1 + \sqrt{1 + \pi\frac{L}{\beta^2 m^2}}}\right)\right] \qquad (15)$$

Test	Load, A/m^2	Time-to-Failure, min.
T1	2	720.9
T2	3	474.5
T3	4	350.5
T4	6	225.3
T5	7	189.6
T6	8	162.6
T7	12	97.8
T8	13	87.1
T9	14	77.8
T10	16	62.4

Table 1: Lifetimes for Constant Loads.

Simulated		*Our Model*			*Peukert's Law*		
test	min.	min.	err.(%)	err.(min.)	min.	err.(%)	err.(min.)
T1	720.9	753.2	4.5	32.3	728.0	1.0	7.1
T2	474.5	490.4	3.4	15.9	467.9	1.4	6.6
T3	350.5	359.0	2.4	8.5	341.9	2.5	8.6
T4	225.3	227.6	1.0	2.3	219.8	2.4	5.5
T5	189.6	190.1	0.3	0.5	185.8	2.0	3.8
T6	162.6	161.9	0.4	0.7	160.6	1.2	2.0
T7	97.8	96.3	1.5	1.5	103.2	5.5	5.4
T8	87.1	86.2	1.0	0.9	94.6	8.6	7.5
T9	77.8	77.5	0.4	0.3	87.2	12.1	9.4
T10	62.4	63.4	1.6	1.0	75.4	20.8	13.0

Table 2: Lifetime Predictions for Constant Loads.

The Peukert's law is given below for reference:

$$a = I^b L \qquad (16)$$

Before the proposed model can be used, we need to estimate the quantities α and β from experimental data. Experiments with constant loads are *sufficient* for estimation purposes. We used the lithium cell simulator DUALFOIL [5, 8] for a rechargeable lithium-ion battery (see [1] for the comparison of the output this low-level simulator with the actual measurements). To cover sufficient range of currents we simulated ten constant loads resulting in the discharge times between 1 hour and 12 hours. The open-circuit voltage is $V_{oc} = 4.31V$, and the cutoff voltage is set to $V_{cutoff} = 3.19V$. The time when the battery voltage drops below V_{cutoff} is considered to be the battery time-to-failure. The results are summarized in Table 1.

Since equation 15 is hard to solve for L, we assume that L is given and try to predict the value of I instead. Using a standard least-squares estimation routine, we fit the data from Table 1 to our model and, for comparison purposes, to the Peukert's law. We obtained the following estimates of the coefficients:

- $\alpha = 271.47$ and $\beta = 10.39$ (our model)
- $a = 1550.2$ and $b = 1.09$ (Peukert's law)

The lifetime predictions, based on equations 15 and 16 with the estimated coefficients, are presented in Table 2. In terms of maximum and average errors, the proposed model fits the data better than the Peukert's model. The maximum error for our model and the Peukert's law are 5% and 21%, respectively. The average error for our model and the Peukert's law are 2% and 6%, respectively.

3.2 General case: variable load

We approximate the time-varying discharge rate by a piece-wise constant load. Figure 2 shows an example of such an approximation. Let $U(t)$ denote the step function. Recall that $U(t) = 1$ if $t \geq 0$, while $U(t) = 0$ for $t < 0$. In the interval $[0,t]$, the variable

load $i(t)$ can be expressed as an n-step staircase function:

$$i(t) = \sum_{k=1}^{n} I_{k-1}[U(t-t_{k-1}) - U(t-t_k)] \tag{17}$$

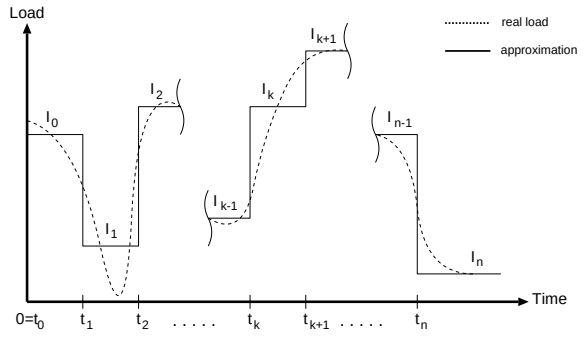

Figure 2: Staircase Approximation of Variable Load.

After substitution of $i(t)$ into equation 11 and integrating the n-term sum term by term, we obtain:

$$\begin{aligned}\alpha = \quad & \textstyle\sum_{k=1}^{n} \int_0^L \frac{I_{k-1}[U(\tau-t_{k-1})-U(\tau-t_k)]}{\sqrt{L-\tau}}\, d\tau + \\ & 2\textstyle\sum_{m=1}^{\infty}\sum_{k=1}^{n} \int_0^L \frac{I_{k-1}[U(\tau-t_{k-1})-U(\tau-t_k)]}{\sqrt{L-\tau}}\, e^{-\frac{\beta^2 m^2}{L-\tau}}\, d\tau\end{aligned} \tag{18}$$

Next, we change the integration limits to drop the step functions:

$$\alpha = \sum_{k=1}^{n} I_{k-1}\left[\int_{t_{k-1}}^{t_k} \frac{d\tau}{\sqrt{L-\tau}} + 2\sum_{m=1}^{\infty}\int_{t_{k-1}}^{t_k} e^{-\frac{\beta^2 m^2}{L-\tau}} \frac{d\tau}{\sqrt{L-\tau}}\right] \tag{19}$$

Then,

$$\begin{aligned}\alpha = \quad & \textstyle\sum_{k=1}^{n} 2I_{k-1}\Big\{\sqrt{L-t_{k-1}} - \sqrt{L-t_k} + \\ & 2\textstyle\sum_{m=1}^{\infty}\Big[\sqrt{L-t_{k-1}}\, e^{-\frac{\beta^2 m^2}{L-t_{k-1}}} - \sqrt{L-t_k}\, e^{-\frac{\beta^2 m^2}{L-t_k}} - \\ & \beta m\sqrt{\pi}\bar{\Phi}\left(\tfrac{\beta m}{\sqrt{L-t_{k-1}}}\right) + \beta m\sqrt{\pi}\bar{\Phi}\left(\tfrac{\beta m}{\sqrt{L-t_k}}\right)\Big]\Big\}\end{aligned} \tag{20}$$

Let $A(L,t_k,t_{k-1},\beta)$ represent the factor by which $2I_{k-1}$ is multiplied. Similarly to the constant load case, we obtain the following relationship between the time-to-failure L and the variable load $i(t)$, approximated in the interval $[0,L]$ by an n-step staircase function:

$$\boxed{\alpha = \sum_{\mathbf{k=1}}^{\mathbf{n}} \mathbf{2I_{k-1}A(L,t_k,t_{k-1},\beta)}} \tag{21}$$

$$\begin{aligned}A(L,t_k,t_{k-1},\beta) = & \\ & \sqrt{L-t_{k-1}}\left[1 + 2\textstyle\sum_{m=1}^{10}\left(e^{-\frac{\beta^2 m^2}{L-t_{k-1}}} - \frac{\pi\, e^{-\frac{\beta^2 m^2}{L-t_{k-1}}}}{\pi - 1 + \sqrt{1+\pi\frac{L-t_{k-1}}{\beta^2 m^2}}}\right)\right] \\ & -\sqrt{L-t_k}\left[1 + 2\textstyle\sum_{m=1}^{10}\left(e^{-\frac{\beta^2 m^2}{L-t_k}} - \frac{\pi\, e^{-\frac{\beta^2 m^2}{L-t_k}}}{\pi - 1 + \sqrt{1+\pi\frac{L-t_k}{\beta^2 m^2}}}\right)\right]\end{aligned} \tag{22}$$

For $n = 1$, equation 21 reduces to the special case described by equation 15. It is important to note that $t_0 = 0$ and $t_n = L$.

The extension of Peukert's equation to the variable load case is straight forward: the load is averaged over the interval $[0,L]$. Since the load average depends on L, solving this equation for L becomes difficult. The generalization of the Peukert's law is as follows:

$$a = \left[\frac{\sum_{k=1}^{n} I_{k-1}(t_k - t_{k-1})}{L}\right]^b L \tag{23}$$

Equation 23 is not as simple as it looks: note that the unknown L appears inside the n-term sum as well, since $t_n = L$. For $n = 1$, equation 23 reduces to equation 16.

The experimental results for the variable load are presented in Section 4. We compare our model not only to the simulation results but also to the generalized Peukert's law.

4. EXPERIMENTAL RESULTS

In this section we describe several experiments performed with the DUALFOIL simulator and compare the simulated lifetimes with our predictions. The purpose of these experiments is to see how robust our model is and how changes in load profiles affect the battery lifetime. We use equations 15 and 21 to compute the time-to-failure L of the battery under constant loads and variable loads, respectively. Our procedure for finding L is described in Section 5. Besides giving lifetimes due to our model, we also compute Peukert's predictions. We let the simulator and the model operate with the same description of the load to avoid errors associated with the load approximation. The time-to-failure is computed with the accuracy of 0.1 minute.

Table 3 summarizes the experiments. The first column indicates the load values; while the second column specifies the durations of the corresponding load values. The first five cases are constant loads, ranging from $1A/m^2$ to $20A/m^2$. The purpose of these five experiments is to find the range of loads for which the model works well. The next four cases are interrupted constant loads. For these cases, let L^* denote the lifetime under corresponding continuous load; we discharge the battery for $\frac{3}{4}L^*$ and let it rest for $\frac{1}{4}L^*$ before switching the current back on. The purpose of these four experiments is to expose the recovery effect. The last six cases are variable loads with different timing characteristics. We tested non-periodic and periodic loads followed by a constant rate discharge as well as a pulsed load and a linear load. For periodic loads, information inside { } describes the first period. For example, Case C12 refers to the following load profile. Ten 12.5-minute long periods are applied before the battery starts discharging at the constant rate of $9.6A/m^2$ from the 125th minute on. Within each period, $20A/m^2$ is applied for the first 1.5 minutes, $15A/m^2$ is applied for the next 2 minutes, $10A/m^2$ is applied for another 3 minutes, and $5A/m^2$ is aplied for the last 6 minutes. In Case C15, the load starts at $1A/m^2$ and increases by $0.2A/m^2$ every minute.

Case	Profile, A/m^2	Timing, min.
C1	1	$[0,\infty)$
C2	5	$[0,\infty)$
C3	10	$[0,\infty)$
C4	15	$[0,\infty)$
C5	20	$[0,\infty)$
C6	5-0-5	$[0,206.5)$-$[206.5,275.3)$-$[275.3,\infty)$
C7	10-0-10	$[0,93.2)$-$[93.2,124.3)$-$[124.3,\infty)$
C8	15-0-15	$[0,52.2)$-$[52.2,69.6)$-$[69.6,\infty)$
C9	20-0-20	$[0,31.1)$-$[31.1,41.5)$-$[41.5,\infty)$
C10	20-15-10-5-9.6	$[0,15)$-$[15,35)$-$[35,65)$-$[65,125)$-$[125,\infty)$
C11	5-10-15-20-9.6	$[0,60)$-$[60,90)$-$[90,110)$-$[110,125)$-$[125,\infty)$
C12	{20-15-10-5}-9.6	$\{[0,1.5)$-$[1.5,3.5)$-$[3.5,6.5)$-$[6.5,12.5)\}$-$[125,\infty)$
C13	{5-10-15-20}-9.6	$\{[0,6)$-$[6,9)$-$[9,11)$-$[11,12.5)\}$-$[125,\infty)$
C14	{20-0}	$\{[0,1)$-$[1,2)\}$
C15	1 + 0.2/minute	$[0,\infty)$

Table 3: Load Profiles.

The results of the experiments with the constant loads are shown in Table 4. The maximum and the average errors of our model are 6% and 3%, respectively. Note that the proposed model is accurate within 6% for constant loads with the lifetimes ranging from 1 hour

Simulated		*Our Model*			*Peukert's Law*		
case	min.	min.	err.(%)	err.(min.)	min.	err.(%)	err.(min.)
C1	1459	1542	5.7	83.0	1550	6.2	91.0
C2	275.3	280.1	1.7	4.8	268.3	2.5	7.0
C3	124.3	122.5	1.4	1.8	126.1	1.4	1.8
C4	69.6	70.0	0.6	0.4	81.0	16.4	11.4
C5	41.5	44.0	6.0	2.5	59.2	42.6	17.7

Table 4: Constant Load Lifetimes.

Simulated		*Our Model*			*Peukert's Law*		
case	min.	min.	err.(%)	err.(min.)	min.	err.(%)	err.(min.)
C6	345.9	349.0	0.9	3.1	342.6	1.0	3.3
C7	158.2	154.7	2.2	3.5	159.6	0.9	1.4
C8	92.5	90.0	2.7	2.5	99.9	8.0	7.4
C9	57.5	57.3	0.3	0.2	70.5	22.6	13.0

Table 5: Interrupted Load Lifetimes.

to 1 day. The Peukert's model performed poorly for the heavy loads (see Cases C4 and C5). The maximum and the average Peukert's error are 43% and 14%, respectively.

The results of the experiments with the interrupted loads are shown in Table 5. The simulation values in Table 5 should be compared with the corresponding entries in Table 4 multiplied by $1\frac{1}{4}$. (Cases C6, C7, C8, and C9 correspond to Cases C2, C3, C4, and C5, respectively.) If recovery takes place, the lifetimes in Table 4 should be extended by more than 25% (the duration of the rest period). Table 6 shows the lifetime L^* under a continuous load, the lifetime $1.25L^*$ under an interrupted load when there is no recovery, the actual lifetime L observed under that interrupted load, and the percentage of L^* gained due to recovery. Cases C6-C9 indicate that the higher the load, the greater the recovery effect. Under such interrupted loads the time-to-failure can be extented by more than 13%. Our model predicted lifetimes within 3% error margin, with the average error of 2%. The Peukert's law produced less accurate prediction with the maximum error exceeding 20% and the average error of 8%.

The results of the experiments with the variable loads are shown in Table 7. As the lifetimes of Cases C10 and C11 indicate, not only load values but also load schedules affect the battery behavior. Note that it may be beneficial to schedule non-periodic loads in non-increasing order of their values: the battery handle high loads better at the beginning than in at the end of discharge. The non-increasing ordering in Case C10 results in the longer lifetime than that of Case C11. Such an ordering may be beneficial for periodic loads as well (see Cases C12 and C13). According to Cases C11 and C13, converting a non-periodic load into a periodic load may also extend the time-to-failure of the battery.

Case C14 demonstrate that load relaxation may have a significant positive effect. The battery was subjected to the pulsed load with the period of 2 minutes and 50% duty cycle. Within each period, the heavy load of $20A/m^2$ is followed by an off-line rest. Recall that under the continuous load of $20A/m^2$ the battery fails in less than 42 minutes. Due to recovery, the battery was able to service

Case	L^*, minutes	$1.25L^*$, minutes	L, minutes	Recovery, %
C6	275.3	344.1	345.9	0.7
C7	124.3	155.4	158.2	2.3
C8	69.6	87.0	92.5	7.9
C9	41.5	51.9	57.5	13.5

Table 6: Recovery Effect under Interrupted Loads.

Simulated		*Our Model*			*Peukert's Law*		
case	min.	min.	err.(%)	err.(min.)	min.	err.(%)	err.(min.)
C10	133.8	133.7	0.1	0.1	131.8	1.5	2.0
C11	115.4	113.5	1.6	1.9	131.8	14.2	16.4
C12	131.0	131.2	0.2	0.2	131.8	0.6	0.8
C13	123.5	123.6	0.1	0.1	131.8	6.7	8.3
C14	113.0	114.8	1.6	1.8	125.0	10.6	12.0
C15	93.6	92.7	1.0	0.9	107.1	14.4	13.5

Table 7: Variable Load Lifetimes.

57 minutes of $20A/m^2$, which translates into the lifetime gain of more than 30%.

For Cases C10-C15, the average error of the Peukert's predictions is 8%, with the maximum error exceeding 14%. Not surprisingly, the Peukert's law did not account for any lifetime variations in Cases C10-C13. Our model, on the other hand, not only captured the trend in the battery behavior, but also produced results with the average error less than 1% and the maximum error of 2%.

5. MODEL APPLICATION

In this Section we outline the main issues related to applicability of the proposed model. Besides lifetime estimation, our model can be used as a cost function for load schedule synthesis.

5.1 Lifetime estimation

Given the n-step staircase approximation of a load profile, first, we want to know at which step the battery dies, and second, we want to find the time-to-failure within the interval of that step. We introduce two ordered sets for load values and their timing: $S_I = (I_0, I_1, ..., I_n)$ and $S_t = (t_0, t_1, ..., t_n)$ (see Figure 2; $t_0 = 0$). Our goal can be achieved by executing the procedure shown in Figure 3. The input is the model parameters α and β as well as the sets S_I and S_t. The output is a two-element set: the first element is the time-to-failure found, and second element is either zero, or the difference between the n-term sum and α in equation 21. The time-to-failure is infinite, if the battery does not die before or at t_n. In this case, the difference between the n-term sum and α is returned. It can tell us how well the battery is surviving: the smaller the difference, the greater the need for recovery. If the battery dies before or at t_n, the procedure returns zero along with the specific value of the time-to-failure.

Lifetime Estimation $(S_I, S_t, \alpha, \beta)$
  IF $\alpha < 2I_0A(t_1, t_1, 0, \beta)$,
    Find the smallest $t \in [0, t_1]$ such that:
      $\alpha < 2I_0A(t, t, 0, \beta)$
    RETURN $\{t,\ 0\}$
  Find the smallest integer $u \in \{2, 3, ..., n\}$ such that:
    $\alpha < \sum_{k=1}^{u} 2I_{k-1}A(t_u, t_k, t_{k-1}, \beta)$
  IF u is not found,
    RETURN $\{\infty,\ \alpha - \sum_{k=1}^{n} 2I_{k-1}A(t_n, t_k, t_{k-1}, \beta)\}$
  Find the smallest $t \in [t_{u-1}, t_u]$ such that:
    $\alpha < \sum_{k=1}^{u-1} 2I_{k-1}A(t, t_k, t_{k-1}, \beta) + 2I_{u-1}A(t, t, t_{u-1}, \beta)$
  RETURN $\{t,\ 0\}$

Figure 3: Lifetime Estimation.

Let ΔT denote the duration of a single step in the staircase approximation of the variable load. For the sake of simplicity, assume that ΔT is the same during the entire discharge process. Let Δt denote the smallest time unit in terms of which the time-to-failure is expressed. Also, let ΔT be a multiple of Δt. Then, once the failing step u is determined, it takes $O(n\frac{\Delta T}{\Delta t})$ to find the lifetime within

$[t_u, t_u + \Delta T]$. In order to find the failing step u, one must check the values of the u-term sum at most n times; therefore, finding u will take $O(n^2)$. The overall complexity is $O(n^2 + n\frac{\Delta T}{\Delta t})$. For a given load profile, the value of n is determined by ΔT. The value of ΔT and Δt can be chosen so that the accuracy is traded off for computational delay. (In order to control the growth of the set sizes $|S_I|$ and $|S_t|$ as time increases, one can adjust the value of ΔT accordingly.)

5.2 Lifetime optimization

As we have noted in Section 4, it may be beneficial to schedule loads in the non-decreasing order of their values. Given a set of tasks with the corresponding load values and their durations, we can construct a load sequence that follows this preliminary guideline. Moreover, we can take advantage of the recovery effects by scheduling rest periods.

Scheduling decisions can be based on the value of the difference between the n-term sum and α in equation 21. (For the battery to be alive, the sum must always be less than or equal to α.) The formulation of the lifetime optimization problem is shown in Figure 4. Let the dependencies among tasks be represented by a task graph G. The input is the task graph G, the delay budget B, the *unordered* set S_I^* of the load values for each task, and the corresponding set S_t^* of task durations. The output is the *ordered* set S_I of the load values and the corresponding timing set S_t. If some number of the rest periods are scheduled, then the set S_I will also contain the same number of zero-entries, and the set S_t will contain the corresponding timing information. (Note that inserting the rest periods increases the overall application execution delay.) The objective is to maximize the difference between the sum $\sum_{k=1}^{n} 2I_{k-1}A(t_n, t_k, t_{k-1}, \beta)$ and α. The constraints are as follows:

1. task dependencies are preserved,
2. the latency does not exceed the delay constraint, and
3. at any time within a schedule, the battery is alive.

PROBLEM: Lifetime Maximization
INPUT: G, S_I^*, S_t^*
OUTPUT: S_I, S_t
OBJECTIVE: $\max\{\alpha - \sum_{k=1}^{n} 2I_{k-1}A(t_n, t_k, t_{k-1}, \beta)\}$
CONSTRAINTS:
1) $\forall\, I_p, I_q$, if I_q depends on I_p, then $t_p < t_q$
2) $t_n \leq B$
3) $\forall\, u \leq n$, $\sum_{k=1}^{u} 2I_{k-1}A(t_u, t_k, t_{k-1}, \beta) \leq \alpha$

Figure 4: Lifetime Maximization Problem.

Direct computation of the cost function will take $O(n)$, and explicit checking that the battery is alive within the schedule latency (the third constraint) will take $O(n^2)$.

6. CONCLUSION

We described the analytical model for the lithium-ion batteries for portable electronic systems. The proposed model not only allows a designer to predict the battery time-to-failure for a given load, but also provides a cost metric for an optimization algorithm that aims at maximization of the battery lifetime. Our model also allows for a tradeoff between the accuracy and the amount of computation performed.

The functional form of the model was derived based on physical principles, and its coefficients were fitted statistically, based on simulation results. The model predictions were compared with the simulation data under the constant discharge, interrupted discharge, and general variable discharge conditions (these tests resulted in the lifetimes ranging from 0.1 hours to 1 day). The average error of our predictions for these cases was within 3%.

7. REFERENCES

[1] P. Arora, M. Doyle, A. Gozdz, R. White, and J. Newman. Comparison between computer simulations and experimental data for high-rate discharges of plastic lithium-ion batteries. *J. Power Sources*, (88), 2000.

[2] A. Bard and L. Faulkner. *Electrochemical Methods.* Wiley, New York, 1980.

[3] L. Benini, G. Castelli, A. Macii, E. Macii, M. Poncino, and R. Scarsi. A discrete-time battery model for high-level power estimation. *Proc. DATE*, 2000.

[4] P. Borjesson and C. Sundberg. Simple approximations for the error function q(x) for communications applications. *IEEE Trans. Communications*, March 1979.

[5] M. Doyle, T. Fuller, and J. Newman. Modeling of galvanostatic charge and discharge of the lithium/polymer/insertion cell. *J. Electrochemical Society*, 140(6), 1993.

[6] M. Doyle and J. Newman. Modeling the performance of rechargeable lithium-based cells: design correlations for limiting cases. *J. Power Sources*, (54), 1995.

[7] D. L. (editor). *Handbook of Batteries*. McGraw-Hill, New York, 1995.

[8] T. Fuller, M. Doyle, and J. Newman. Simulation and optimization of the dual lithium ion insertion cell. *J. Applied Electrochemistry*, 141(1), 1994.

[9] S. Gold. A pspice macromodel for lithium-ion batteries. *Proc. Battery Conference*, 1997.

[10] I. Gradshteyn and I. Ryzhik. *Table of Integrals, Series, and Products.* Academic Press, New York, 1965.

[11] T. Martin and D. Siewiorek. The impact of battery capacity and memory bandwidth on cpu speed-setting: a case study. *Proc. ISLPED*, 1999.

[12] D. Panigrahi, C. Chiasserini, S. Dey, R. Rao, A. Raghunathan, and K. Lahiri. Battery life estimation of mobile embedded systems. *Proc. VLSI Design*, 2001.

[13] M. Pedram and Q. Wu. Design considerations for battery-powered electronics. *Proc. DAC*, 1999.

[14] G. Roberts and H. Kaufman. *Table of Laplace Transforms.* Saunders, Philadelphia, 1966.

[15] T. Simunic, L. Benini, and G. D. Micheli. Energy-efficient design of battery-powered embedded systems. *Proc. ISLPED*, 1999.

[16] K. Syracuse and W. Clark. A statistical approach to domain performance modeling for oxyhalide primary lithium batteries. *Proc. Battery Conference*, 1997.